Supplementary Information

Mengyao Chen[1†], Xiangying Shen[1,2,3,4†], Zhen Chen[1],
Jack Hau Yung Lo[1], Yuan Liu[1], Xinliang Xu[3], Lei Xu[1,4]

1. The Department of Physics, The Chinese University of Hong Kong, Shatin, Hong Kong, China

[2] *Department of Materials Science and Engineering, Southern University of Science and Technology, Shenzhen, China*

[3] *The Beijing Computational Science Research Center, Beijing, China*

[4] *Shenzhen Research Institute, The Chinese University of Hong Kong, Shenzhen, China*

(Dated: September 9, 2022)

I. TRANSFORMED PERMEABILITY TENSORS OF THE CLOAK, CONCENTRATOR AND ROTATOR

In this section, we give the brief analysis about the transformed permeability tensors of the cloak, concentrator and rotator in flow field. We will see all these three tensors can be written in the same form of $S\text{diag}(k_r, k_\theta)S^{-1}$.

Without loss of the generality, as shown in Fig.S1, assume the two dimensional space in the polar coordinate system (r, θ) is divided by a shell-shaped metamaterial into three regions: region I ($r < a$), the area inside the metamaterial; region II ($a < r < b$), the metamaterail shell itself; region III ($r > b$), the area outside the metamaterial. According to the transformation mapping theory, to achieve the cloaking effect, the corresponding coordinate transformation is:

$$\begin{cases} r' = a + r(b-a)/b, \\ \theta' = \theta, \end{cases} \tag{1}$$

Under such a transformation, the domain equation (Eq.(1) in the main text) remains form invariant while the permeability tensor becomes $\mathbf{k} = k_0 T = k_0 J J^{\mathrm{T}}/\det(J)$, where k_0 is the background's permeability and

$$J = \partial(r', \theta')/\partial(r, \theta) = \begin{pmatrix} \dfrac{\partial r'}{\partial r} & \dfrac{\partial r'}{\partial \theta} \\ \\ \dfrac{\partial \theta'}{\partial r} & \dfrac{\partial \theta'}{\partial \theta} \end{pmatrix}, \tag{2}$$

is the Jacobian matrix. In fact, for the cloak transformation, three steps are involved: First, the cartesian coordinate system are transformed into the polar system; Next, following the transformation in Eq. (1), the circle region within $r < b$ are mapped into the annulus area $a < r < b$; Last, the mapped polar coordinates are transformed back into the cartesian system. This compound coordinate transformation is expressed as: $(x, y) \to (r, \theta) \to (r', \theta') \to (x', y')$. The corresponding Jacobian matrix is written as:

$$\begin{aligned} J_{xx'} &= J_{xr} J_{rr'} J_{r'x'} \\ &= R(\theta)\text{diag}(1, r)\text{diag}(\frac{b-a}{b}, 1)\text{diag}(1, 1/r')R(\theta), \\ &= R(\theta)\text{diag}(\frac{b-a}{b}, r/r')R(\theta) \end{aligned} \tag{3}$$

where $R(\theta)$ is the rotation matrix and

$$\begin{aligned} J_{xr} &= \partial(x,y)/\partial(r,\theta) \\ J_{rr'} &= \partial(r,\theta)/\partial(r',\theta') \\ J_{r'x'} &= \partial(r',\theta')/\partial(x',y') \end{aligned} \quad . \tag{4}$$

In consideration of $R(\theta)^{-1} = R(\theta)^{\mathrm{T}}$, the transformed matrix T can be calculated as:

$$\begin{aligned} T &= J_{xx'}^{-\mathrm{T}} J_{xx'}^{-1} \det(J_{xx'}) \\ &= R(\theta)^{-\mathrm{T}} \mathrm{diag}(\frac{b-a}{b}, r'/r) R(\theta) \\ & R(\theta)^{-1} \mathrm{diag}(\frac{b-a}{b}, r'/r) R(\theta)^{-1} \frac{rb}{r'(b-a)}, \\ &= R(\theta) \mathrm{diag}(\frac{r'-a}{r'}, \frac{r'}{r'-a}) R(\theta)^{-1} \\ &= R(\theta) \mathrm{diag}(k_r, k_\theta) R(\theta)^{-1} \end{aligned} \tag{5}$$

which is conform to the form $S\mathrm{diag}(k_r, k_\theta)S^{-1}$.

To concentrate the flow inside the metamaterial without disturbing the outside, a virtual radius $a < c < b$ must be introduced, and the coordinate transformation is given as:

$$\begin{cases} r' = \dfrac{a}{c} r, (0 \le r \le c) \\ r' = \dfrac{b-a}{b-c} r + \dfrac{a-c}{b-c} b, (c \le r \le b) \\ \theta' = \theta. \end{cases} \tag{6}$$

Similar to the cloak case, we can derive T for the concentrator:

$$\begin{aligned} T &= J_{xx'}^{-\mathrm{T}} J_{xx'}^{-1} \det(J_{xx'}) \\ &= R(\theta) \mathrm{diag}(k_r, k_\theta) R(\theta)^{-1} \end{aligned}, \tag{7}$$

where

$$\begin{cases} k_r = 1, \;\; k_\theta = 1 \;\; (0 \le r \le c) \\ \\ k_r = \dfrac{r' + b(c-a)/(b-c)}{r'}, \;\; k_\theta = \dfrac{r'}{r' + b(c-a)/(b-c)} \;\; (c \le r \le b) \end{cases} \tag{8}$$

Apparently, the permeability tensor of the concentrator is also in the form of $S\mathrm{diag}(k_r, k_\theta)S^{-1}$.

The coordinate transformation for the rotator is:

$$\begin{cases} r' = r \\ \theta' = \theta + \theta_0 \dfrac{f(b) - f(r)}{f(b) - f(a)}. \end{cases} \tag{9}$$

Here $f()$ can be any continuous function. For simplicity, we set $f(x) = x$. Then the transformation is simplified to $\theta' = \theta + \theta_0(b-r)/(b-a)$. The transformation matrix reads:

$$\begin{aligned} T &= J_{xx'}^{-\mathrm{T}} J_{xx'}^{-1} \det(J_{xx'}) \\ &= R(\theta) \begin{pmatrix} 1 & -t \\ -t & 1+t^2 \end{pmatrix} R(\theta)^{-1}, \end{aligned} \tag{10}$$

where $t = \theta_0/(b-a)$. It should be noted that the matrix between the rotation matrices is symmetric, so that it can be further diagonolized as

$$\begin{pmatrix} 1 & -t \\ -t & 1+t^2 \end{pmatrix} = P \begin{pmatrix} \frac{1}{2}\left(2+t^2-t\sqrt{4+t^2}\right) & 0 \\ 0 & \frac{1}{2}\left(2+t^2+t\sqrt{4+t^2}\right) \end{pmatrix} P^{-1}, \tag{11}$$

where

$$P = \begin{pmatrix} \frac{t+\sqrt{4+t^2}}{2\sqrt{1+(t+\sqrt{4+t^2})/4}} & \frac{t-\sqrt{4+t^2}}{2\sqrt{1+(t-\sqrt{4+t^2})/4}} \\ \frac{1}{\sqrt{1+(t+\sqrt{4+t^2})/4}} & \frac{1}{\sqrt{1+(t-\sqrt{4+t^2})/4}} \end{pmatrix}. \tag{12}$$

Therefore, the permeability tensor of the rotator can also be written as $S\mathrm{diag}(k_r, k_\theta)S^{-1}$, where $S = R(\theta)P$. In the polar coordinate system the three metamaterials' permeability tensor are given below:

$$\mathbf{k}_{cloak} = k_0 \begin{pmatrix} \frac{r'-a}{r'} & 0 \\ 0 & \frac{r'}{r'-a} \end{pmatrix} \ (a<r<b),$$

$$\mathbf{k}_{concen} = k_0 \begin{pmatrix} \frac{r'+b(c-a)/(b-c)}{r'} & 0 \\ 0 & \frac{r'}{r'+b(c-a)/(b-c)} \end{pmatrix} \ (c<r<b), \tag{13}$$

$$\mathbf{k}_{rot} = k_0 P \begin{pmatrix} \frac{1}{2}\left(2+t^2-t\sqrt{4+t^2}\right) & 0 \\ 0 & \frac{1}{2}\left(2+t^2+t\sqrt{4+t^2}\right) \end{pmatrix} P^{-1} \ (a<r<b),$$

II. THE DOMAIN EQUATION FOR COMPRESSED OR EXTENDED SPACE

According to the last section, the cloaking, concentrating and rotating effects are essentially the compression, extension and rotation operations on the original space without changing

the determinant of the original permeability tensor. In fact, the diagonal transformed tensor of the cloak and concentrator induced by compression and extension, respectively, can be further reduced to $\mathrm{diag}(n^2, 1/n^2)$, where n is a constant independent of r and θ. $|n| < 1$ for compression, and $|n| > 1$ for extension [1, 2].

Next, we will see how the compression and extension operation manipulate the internal flow's rate. The Darcy's pressure equation [3, 4] given in the main text reads:

$$-\vec{\nabla} \cdot \mathbf{k} \cdot \vec{\nabla} P = 0. \tag{14}$$

Under the coordinate transformation, the above equation changes to

$$-\frac{1}{\sqrt{|g|}} \partial_u (\mathbf{k} \sqrt{|g|} g^{uv} \partial_v P) = 0, \tag{15}$$

where g_{uv} is the metric tensor, $g = \det(g_{uv})$, and as g is a diagonal matrix, $g^{uv} = g_{uv}^{-1}$. For two dimensional polar coordinate system,

$$g_{uv} = \begin{pmatrix} 1 & 0 \\ 0 & r^2 \end{pmatrix}, \tag{16}$$

and $g = r^2$. Taking the $\mathbf{k} = \mathrm{diag}(n^2, 1/n^2)$ into the Eq. (15), we have

$$\begin{aligned}
&\vec{\nabla} \cdot \mathbf{k} \cdot \vec{\nabla} P \\
&= \frac{1}{\sqrt{|g|}} \partial_u (\mathbf{k} \sqrt{|g|} g^{uv} \partial_v P) = \frac{1}{r} \partial_u (\mathbf{k} r g^{uv} \partial_v P) \\
&= \frac{1}{r} \partial_r (n^2 r g^{rr} \partial_r P) + \frac{1}{r} \partial_\theta (\frac{r}{n^2} g^{\theta\theta} \partial_\theta P) \\
&= \frac{1}{r} \partial_r (n^2 r \partial_r P) + \frac{1}{r} \partial_\theta (\frac{r}{n^2} \partial_\theta P) \\
&= n^2 \frac{\partial^2 P}{\partial r^2} + \frac{n^2}{r} \frac{\partial P}{\partial r} + \frac{1}{n^2 r^2} \frac{\partial^2 P}{\partial \theta^2} = 0.
\end{aligned} \tag{17}$$

III. HOW COMPRESSION AND EXTENSION OPERATIONS MANIPULATE THE INTERNAL FLOW'S MAGNITUDE?

We demonstrate how compression and extension operations manipulate the internal flow's magnitude: because $\mathbf{k}_j = \mathrm{diag}(k_{r,j}, k_{\theta,j})$ with $k_{r,j}$ and $k_{\theta,j}$ being constants independent of r, θ, we can write Eq. (14) in the polar coordinate system as(see section III in SI for details):

$$\frac{\partial^2 P}{\partial r^2} + \frac{1}{r} \frac{\partial P}{\partial r} + \frac{k_{\theta,j}}{k_{r,j}} \frac{\partial^2 P}{r^2 \partial \theta^2} = 0. \tag{18}$$

Suppose that the flow goes from the left to the right with a pressure difference P_0 across a distance L. There are impermeable walls at the top and bottom boundaries of the porous medium. In Darcy's law, although the no-slip boundary condition causes a correction and cannot be strictly satisfied, in most practical situations this correction is small [10, 11]. In some commercial finite elemental analysis software such as COMSOL, the impermeable walls are always set to satisfy the no-slip boundary condition. Thus, this approximation is also adopted in our analysis. L is the dimension of the system in the flow direction along x axis and P_0/L is the pressure gradient in background. Considering the symmetry relation of $P(r,\theta) = P(r,-\theta)$, the general solution of Eq. (18) in three regions can be expressed as:

$$P_j = \sum_{n=1}^{\infty} \left[A_{2n-1}^j r^{(2n-1)\sqrt{k_{\theta,j}/k_{r,j}}} + B_{2n-1}^j r^{-(2n-1)\sqrt{k_{\theta,j}/k_{r,j}}} \right] \cos(2n-1)\theta, \tag{19}$$

The pressure in the far field $r \to \infty$ needs to match the background pressure $-\frac{P_0}{L} r\cos\theta$. As a result, we only need to consider the $n = 1$ case. At the origin $r = 0$, P_1 should be finite thus $B_1^1 = 0$. Thus we obtain the solutions in different regions as:

$$\begin{aligned} P_1 &= A_1^1 r\cos\theta, \\ P_2 &= \left[A_1^2 r^{\sqrt{k_{\theta,2}/k_{r,2}}} + B_1^2 r^{-\sqrt{k_{\theta,2}/k_{r,2}}} \right] \cos\theta, \\ P_3 &= [A_1^3 r + B_1^3 r^{-1}] \cos\theta, \end{aligned} \tag{20}$$

With the boundary conditions of continuous pressure and radial velocity at the interface of different regions:

$$\begin{aligned} &P_1|_{r=a} = P_2|_{r=a}, \\ &P_2|_{r=b} = P_3|_{r=b}, \\ &k_{r,1}\tfrac{\partial P_1}{\partial r}|_{r=a} = k_{r,2}\tfrac{\partial P_2}{\partial r}|_{r=a}, \\ &k_{r,2}\tfrac{\partial P_2}{\partial r}|_{r=b} = k_{r,3}\tfrac{\partial P_3}{\partial r}|_{r=b}, \end{aligned} \tag{21}$$

all the pre-factors can be solved and the exact pressure distributions can be derived:

$$\begin{aligned} P_1 &= -\tfrac{P_0}{L}\left(\frac{a}{b}\right)^{h-1} r\cos\theta, \\ P_2 &= -\tfrac{P_0}{L}\left(\frac{r}{b}\right)^{h-1} r\cos\theta, \\ P_3 &= -\tfrac{P_0}{L} r\cos\theta, \end{aligned} \tag{22}$$

where P_1, P_2, P_3 are the pressure distributions in regions I, II, III, $h = \sqrt{k_{\theta,2}/k_{r,2}}$. According to these pressure solutions, in regions I and III we obtain constant velocity along the x axis: $v_{x,j} = k_0 dP_j/dx = constant$. Thus, the ratio between the internal and external flow's velocities is $v_{x,1}/v_{x,3} = (a/b)^{h-1}$, which is determined by the parameters a, b and h.

When $h = 1$, P_1, P_2 and P_3 have the same expression and the shell is completely transparent with respect to the background flow: the entire system can be regarded as a homogenous and isotropic porous medium. When $h < 1$, $v_{x,1}/v_{x,3} = (b/a)^{1-h} > 1$ and the velocity of the internal flow is greater than that of the external flow. When $h > 1$, $v_{x,1}/v_{x,3} = (a/b)^{h-1} < 1$ and the internal flow is smaller than the outer flow. Besides the magnitude, the rotation matrix $\mathbf{R}$ adds another degree of freedom in manipulating the internal flow's direction. Therefore, by designing a proper shell permeability $\mathbf{k}_2$ with an effective permeability $k_{e,2}$ matched to the background permeability k_0, we can control both the magnitude and the direction of the internal flow while making no disturbance to the external flow.

IV. ONE POSSIBLE APPLICATION EXAMPLE OF THE METAMATERIAL DEVICE

What are possible applications of our device? We demonstrate one potential application in its effective control on bacterial biofilm growth [5–8]. To some extent, bacteria can be considered as a simplified model system for many complex living matters, and an effective control over bacteria growth provides direct evidence of possible application in the control of living matter. As shown in Fig.S1(a), we manufacture cloak (left), concentrator (right) and an intermediate structure (middle) inside a background porous medium. They are placed side by side so that the bacteria inside them can grow at the same time and with identical bacteria batch, nutrient condition, temperature, etc. We flow bacteria-carrying fluid from the left inlet to the right outlet with a constant rate of 0.003ml/min and at the temperature of $25°C$. After 15 hours, we compare the biofilm formation indicated by green GFP fluorescence at the center of the three devices, as shown in Fig.S1(b-d). Apparently, the cloak on the left exhibits the largest amount of biofilm while the concentrator on the right shows the least, because the near static environment in cloak facilitates bacteria growth while the strong flow in concentrator flushes the bacteria away. This is quantitatively proved by the total fluorescent intensity shown in Fig.S1(e). Therefore, our device can continuously tune the biofilm growth quantity by tuning the aligning angle β in every other layer ($\beta = 0°, 9°, 18°$ in these three situations).

Besides the quantity, we can also tune the direction of biofilm growth, as shown in Fig.S1(f-j). By manufacturing two different rotators side by side in Fig.S1(f), we realize

the growth of biofilm in opposite directions, as shown clearly in Fig.S1(h) and Fig.S1(i). Moreover, we further prove very little disturbance from the device to the background: two background locations, one far away from and the other close to the rotators, are shown in Fig.S1(g) and Fig.S1(j) and their biofilm growth are identical. This proves unambiguously the little disturbance to the background both far from and close to the device, and the same behavior also appears for cloak and concentrator in Fig.S1(a). Therefore, our device can tune the bacteria growth in both quantity and direction: in case a fast-growing speed is preferred in living matter such as self-healing, the cloak configuration can be chosen; while when a slow-growing speed is preferred such as unclogging, the concentrator configuration can be chosen. With such a continuous tuning ability, our device could fit different needs of living matter control.

One direct application is to build a parallel platform for bacteria or cell culture under various flow conditions, which commonly occur in natural environments. Because of little disturbance to background, devices do not interfere with each other and many of them can combine into one large integrated system, as shown in Fig.S1(k). Thus, each individual device could behave as an independent sub-unit for bacterial (or cell) culture and their combination covers various flow conditions: this integrated system thus becomes a high-efficiency parallel testing and growing platform. Moreover, if each sub-unit couples to its own heating element, both flow and temperature can be adjusted, and an integrated system with two free parameters could be achieved. Therefore, our device could find potential application in the biological area of bacterial or cell culture.

V. THE LEGENDS OF THE SUPPLEMENTARY MOVIES

Movie-1: The flow field in the microfluidic device of the cloak, concentrator and rotator.
Movie-2: The tuning of velocity magnitude and direction in the 3D-printed device.
Movie-3: The flow field in the 3D-printed device of the cloak, concentrator and rotator.

[1] X. Y. Shen, Y. Li, C. R. Jiang, Y. S. Ni, J. P. Huang, "Thermal cloak-concentrator." Applied Physics Letters **109**, 031907 (2016)

[2] X. Y. Shen, C. R. Jiang, Y. Li, J. P. Huang, "Thermal metamaterial for convergent transfer of conductive heat with high efficiency" Applied Physics Letters **109**, 201906 (2016)

[3] Y. A. Urzhumov, D. R. Smith, "Fluid flow control with transformation media." Physical Review Letters **107**, 074501 (2011).

[4] J. Bear. Dynamics of fluids in porous media. Environmental Science. New York - London - Amsterdam: American Elsevier Publishing, 1972.

[5] K. Dreschera, Y. Shen, B. L. Basslera, H. A. Stone, "Biofilm streamers cause catastrophic disruption of flow with consequences for environmental and medical systems." PNAS **110**, 4345 (2013).

[6] A. Valiei, A. Kumar, P. P. Mukherjee, Y. Liud, T. Thundat, "A web of streamers: biofilm formation in a porous microfluidic device." Lab Chip **12** 5133 (2012).

[7] T. F. Mah, B. Pitts, B. Pellock, G. C. Walker, P. S. Stewart, G. A. O'Toole, "A genetic basis for Pseudomonas aeruginosa biofilm antibiotic resistance." Nature **426**, 306 (2003).

[8] M. Whiteley, M. G. Bangera, R. E. Bumgarner, M. R. Parsek, G. M. Teitzel, S. Lory, E. P. Greenberg, "Gene expression in Pseudomonas aeruginosa biofilms." Nature **413**, 860 (2001).

[9] J. W. Costerton, Z. Lewandowski, D. E. Caldwell, D. R. Korber and H. M. Lappinscott, "Microbial biofilms." Annu. Rev. Microbiol **49**, 711 (1995).

[10] D. A. Nield, "The boundary correction for the Rayleigh-Darcy problem: limitations of the Brinkman equation." Journal of Fluid Mechanics **128**, 37 (1983)

[11] D. A. Nield, "Alternative model for wall effect in laminar flow of a fluid through a packed column." AIChE Journal **29**, 688 (1983).

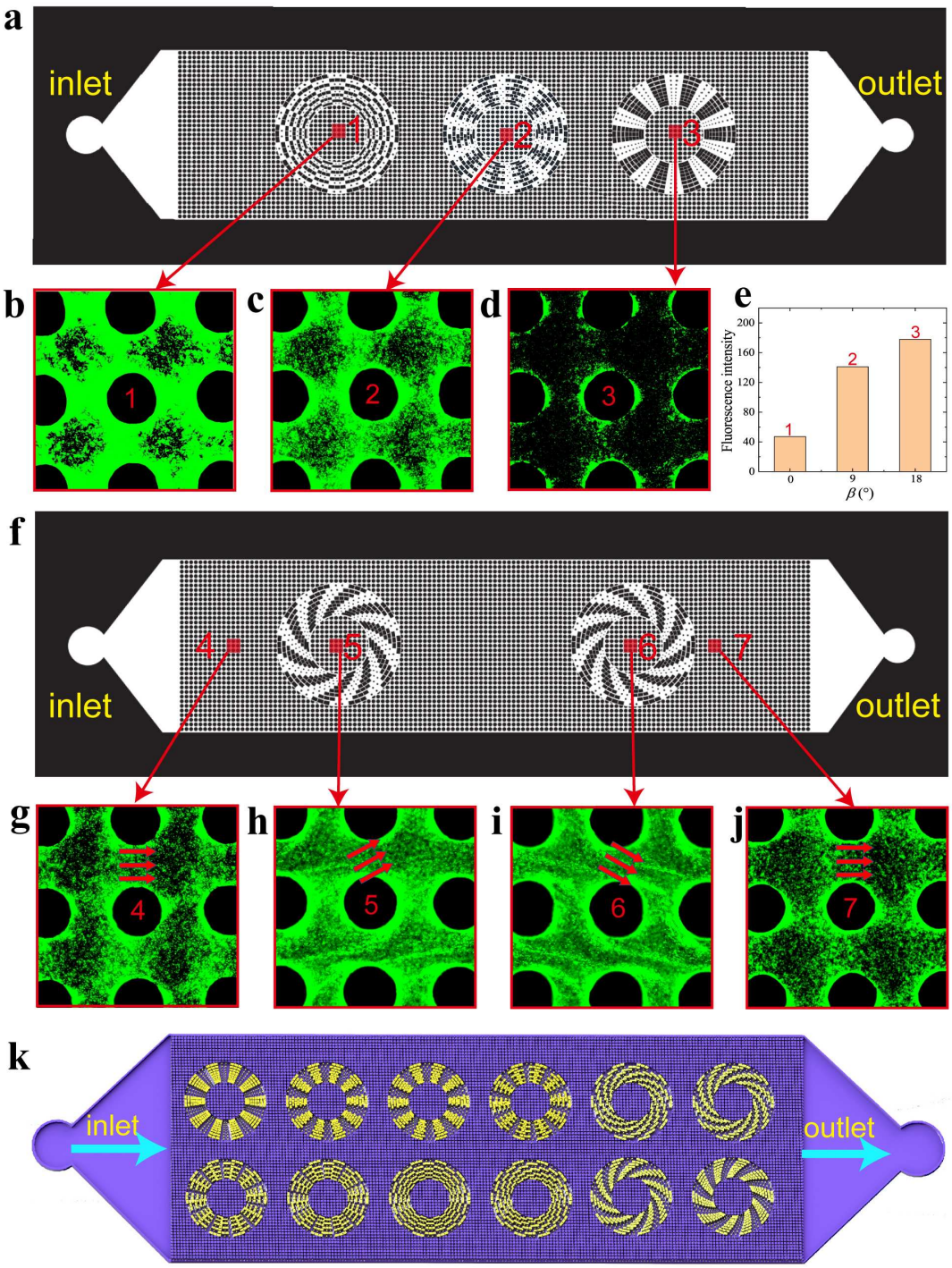

FIG. 1: **a**, the microfluidic device consists three configurations achieved by rotating the angle $\beta = 0°, 9°, 18°$ in every other layer, which corresponds to cloak (left), concentrator (right), and an intermediate structure (middle). **b-d**, the biofilm densities characterized by green fluorescence protein intensity in regions 1, 2, 3 of the device in **a**. **e**, total fluorescence intensity of regions 1, 2, 3. **f**, two opposite rotators with $\alpha = 5°$ and $-5°$ in every layer. **g-j**, the biofilm densities in regions 4, 5, 6, 7 in **f**. Red arrows indicate flow directions. **k**, multiple devices combine to form an integrated large system.